# Development of a Preclinical PET/MRI DOI Detector Using Different Types of Scintillators that Operates in a Magnetic Field

Gyeong Rip Kim<sup>1</sup>, Jong Hyeok Kwak<sup>2\*</sup>, and Seung-Jae Lee<sup>3,4\*</sup>

<sup>1</sup>Department of Neurosurgery, Pusan National University Yangsan Hospital, Yangsan 50612, Republic of Korea <sup>2</sup>Department of Radiology, Pusan National University Yangsan Hospital, Yangsan 50612, Republic of Korea <sup>3</sup>Department of Radiological Science, Dongseo University, Busan 47011, Republic of Korea <sup>4</sup>Center for Radiological Environment & Health Science, Dongseo University, Busan 47011, Republic of Korea

(Received 23 June 2025, Received in final form 29 July 2025, Accepted 30 July 2025)

We developed a high-resolution, preclinical positron emission tomography/magnetic resonance imaging (PET/MRI) detector for measuring depth of interaction (DOI) without signal distortion in a magnetic field. A silicon photomultiplier (SiPM), a semiconductor photosensor, was used to operate in a high magnetic field, and a two-layer scintillator block was fabricated for DOI. The scintillator block used lutetium-yttrium oxyorthosilicate (LYSO) and gadolinium aluminum gallium garnet (GAGG) scintillators, so that the signal sizes acquired form each scintillator layer were different. After constructing the detector, a Na-22 radiation source was used to acquire flood images and energy spectra through gamma-ray interaction. By using different scintillators in each layer, the energy spectrum formed two photoelectric peak areas. Since the signal sizes differ depending on the characteristics of different scintillators, it is possible to determine the DOI layer when data is acquired by separating the photoelectric peak areas. If this detector is used as a DOI detector for preclinical PET/MRI, it will be possible to develop a system with excellent spatial resolution that can operate in a magnetic field.

Keywords: preclinical PET/MRI, magnetic field, semiconductor photosensor, DOI

#### 1. Introduction

Preclinical imaging devices are composed of various imaging devices integrated into one device. Positron emission tomography (PET) and computed tomography (CT) and single photon emission computed tomography (SPECT) and CT are integrated into one device, allowing for acquisition of complementary images [1-3]. Since all of them are imaging devices that use radiation, integration of detectors for acquiring radiation and integration of images can be achieved. In addition to preclinical PET/CT or SPECT/CT, integration of PET/MRI, which integrates PET and magnetic resonance imaging (MRI), is also being achieved. However, in order to obtain PET images in the high magnetic field of MRI, detectors that operate in a conventional method cannot be used. This is because it is difficult to obtain

accurate images due to signal distortion caused by the high magnetic field. Therefore, the need for the development of detectors that operate in high magnetic fields has arisen. In high magnetic fields, electrons moving in the PMT vacuum tube of detectors that use traditional photomultiplier tubes (PMTs) are affected. Accordingly, an photosensor that is not affected by a magnetic field was developed, and this photosensor was introduced into a PET system and used as a radiation detector. The photosensor composed of a semiconductor sensor is not affected by a magnetic field, so it can obtain images without signal distortion. The development of preclinical PET/MRI was also achieved using this optical sensor [4]. In preclinical PET systems, spatial resolution degradation occurs in the periphery of the field of view (FOV). The annihilation radiation generated in the periphery of the FOV is incident on the detector obliquely, so it can interact with multiple scintillation pixels, and thus a line of response (LOR) can be generated from multiple scintillation pixels, which reduces spatial resolution. To solve this problem, a detector that measures the depth of interaction (DOI) is required. Various detectors that measure the DOI have been developed. It can be broadly

©The Korean Magnetics Society. All rights reserved. \*Corresponding author: Tel: +82-55-360-1805 e-mail: kwark9476@naver.com (Jong Hyeok Kwak) \*Corresponding author: Tel: +82-51-320-2719

\*Corresponding author: 1el: +82-51-320-2/19 e-mail: sjlee@gdsu.dongseo.ac.kr (Seung-Jae Lee) classified into three types. The first is a method of stacking multiple layers of scintillation pixel arrays to obtain signals from the interaction between the scintillation pixels of each layer and gamma rays [5-8]. The second is a method of measuring the DOI through the ratio of signals by arranging a single layer of scintillation pixel arrays and photosensors at both ends [9, 10]. The third is a method of configuring a single layer of scintillation pixel arrays and photosensors in one layer, stacking them in multiple layers, and measuring the DOI with gamma rays [11, 12]. In this study, we developed a detector that measures the DOI by stacking multiple layers of scintillation pixel arrays and acquiring signals from the interaction between the scintillation pixels and gamma rays in each layer. Through this, we solved the parallax error, which is a spatial resolution degradation phenomenon in the peripheral FOV that occurs in preclinical PET, and designed it using a semiconductor photosensor so that it can operate in MRI. Scintillators, which are materials that emit light by interacting with radiation, emit light of different wavelengths and generate different amounts of light depending on their type. Based on these characteristics, this detector was developed. By arranging two types of scintillators in layers, the sizes of the signals obtained were made different, allowing the DOI layers to be distinguished. In a previous study, the usability of the designed detector was confirmed through simulation [13]. In this study, a semiconductor photosensor was used to design the sensor so that it is not affected by magnetic fields, and different types of scintillation pixels were configured in two layers. Through experiments, the size of the signal measured in each layer was analyzed to evaluate whether the DOI layer could be measured.

# 2. Materials and Methods

# 2.1. Detector configuration

To design and characterize a detector that can improve spatial resolution in preclinical PET/MRI, a two-layer DOI detector was developed. The detector consists of two layers, and different types of scintillators are used in each layer to enable layer discrimination. The bottom layer used a gadolinium aluminum gallium garnet (GAGG) scintillator, and the top layer used a lutetium-yttrium oxyorthosilicate (LYSO) scintillator. By configuring the amount of light generated in each layer differently, the positions where the photoelectric peaks are formed in the energy spectrum were different. The scintillator of PET detectors that detect high-energy gamma rays of 511 keV must have high density. Therefore, the scintillators of current PET detectors are mainly LYSO or LSO scintillators. In this study, in order to determine the DOI layer through the

separation of the photoelectric peak, another scintillator was used. This scintillator is GAGG, and GAGG has a high density and emits more light than LYSO. Therefore, the two scintillators were designed to distinguish the DOI layer by differentiating the generation positions of the photoelectric peaks. The GAGG scintillator generates 54,000 photons per 1 MeV of gamma-rays, while LYSO generates 30,000 photons [14, 15], so the height of the signals output from the photosensor are different, and the positions where the photoelectric peaks are formed are different. By utilizing these characteristics, the layer where the gammaray interacted with the scintillator can be determined. The detector consists of a 4 × 4 scintillation pixel array in each layer, and the size of the scintillation pixel is 3 mm  $\times$  3 mm  $\times$  10 mm. The space between the scintillation pixels is reflective to maximize the transfer of the generated light to the photosensor. In addition, except for the surface where the scintillation block is coupled to the photosensor, all surfaces are reflective so that all the generated light moves to the photosensor. The reflector reflects the light generated from the scintillator. Since the reflector is inserted between each scintillation pixel, the light generated from the scintillation pixel does not move to other scintillation pixels, but is reflected only within the scintillation pixel and is finally collected by the photosensor. Accordingly, the size of the entire scintillation block is 12.5 mm × 12.5 mm × 20 mm, which is a thickness sufficient to collect highenergy gamma rays. The photosensor uses a silicon photomultiplier (SiPM), a semiconductor photosensor, to operate without distortion in a high magnetic field. Unlike the PMT, a conventional photosensor that uses a vacuum tube, SiPM has a compact size and operates without distortion in a magnetic field, so it can be used in MRI [16]. The SiPM consists of a  $4 \times 4$  array of 3 mm  $\times$  3 mm pixels spaced at 0.2 mm intervals. The scintillator is separated into reflectors in the depth direction, and the light generated in that layer is designed to be incident on the coupled SiPM and the signal is measured. This design allows for a clear separation of the DOI layers. The light generated from the scintillator block travels to the SiPM, where it is collected and converted into an electrical signal. The maximum wavelength of light generated by the GAGG scintillator is 530 nm, and that of the LYSO scintillator is 420 nm. The SiPM has a quantum efficiency of about 40% at the maximum wavelength of light generated by LYSO, and that of GAGG has a quantum efficiency of about 30%. When collecting the maximum light wavelength, the ratio of the size of the electrical signals in the two scintillators is about 1.35 times, and GAGG generates a larger signal, enabling the identification of the layer where the gamma rays interacted. An optical grease is used between

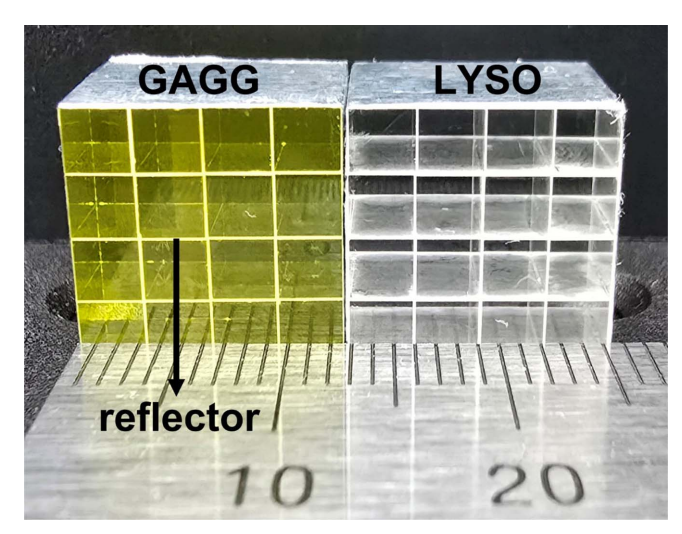


**Fig. 1.** (Color online) Scintillation block of the DOI detector of a preclinical PET/MRI system. GAGG scintillator on the left and LYSO scintillator on the right.

the separation of each scintillator layer and between the scintillator layers and the connection to the SiPM to prevent the occurrence of abrupt refractive indices and minimize light loss. The refractive indices of the scintillator, SiPM, air layer, and optical grease were set to 1.91, 1.57, 1.0, and 1.465, respectively. Fig. 1 shows the scintillator pixel array of each layer constituting the scintillator block. In the diagram of the scintillator pixel array, the GAGG scintillator is on the left, and the LYSO scintillator is on the right. The scintillator pixels are separated by reflectors, so that light is not shared between the scintillator pixels.

#### 2.2. Experimental set-up and data acquisition

To evaluate the detector's DOI layer discrimination

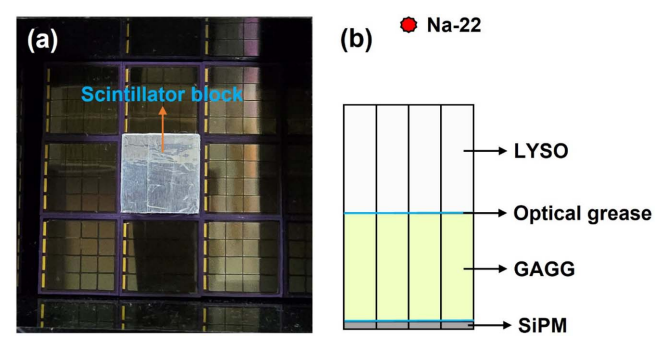


**Fig. 2.** (Color online) Detector configuration and schematic diagram of scintillator block configuration and the location of the radiation source. (a) Combination of the scintillator block and SiPM to form the detector, (b) Na-22 radiation source positioned over the scintillator block to collect data on gamma-ray interactions.

performance, the scintillator block was combined with SiPM, and a radiation source was used to obtain signals due to gamma-ray interaction. The radiation source used was a Na-22 radiation source that generates annihilation radiation through  $\beta$ + decay, and the energy of the emitted gamma-ray is 511 keV. Fig. 2(a) shows the combined appearance of the scintillator block and SiPM, and (b) shows the location of the radiation source. The radiation source was positioned on the scintillator block, and gamma-rays were irradiated onto all scintillation pixels. The light generated by the interaction of gamma-rays and scintillator was collected by SiPM, converted into an electrical signal, amplified by a preamplifier, and then transmitted to a computer through the main board. The computer used the transmitted data to construct images and energy spectra.

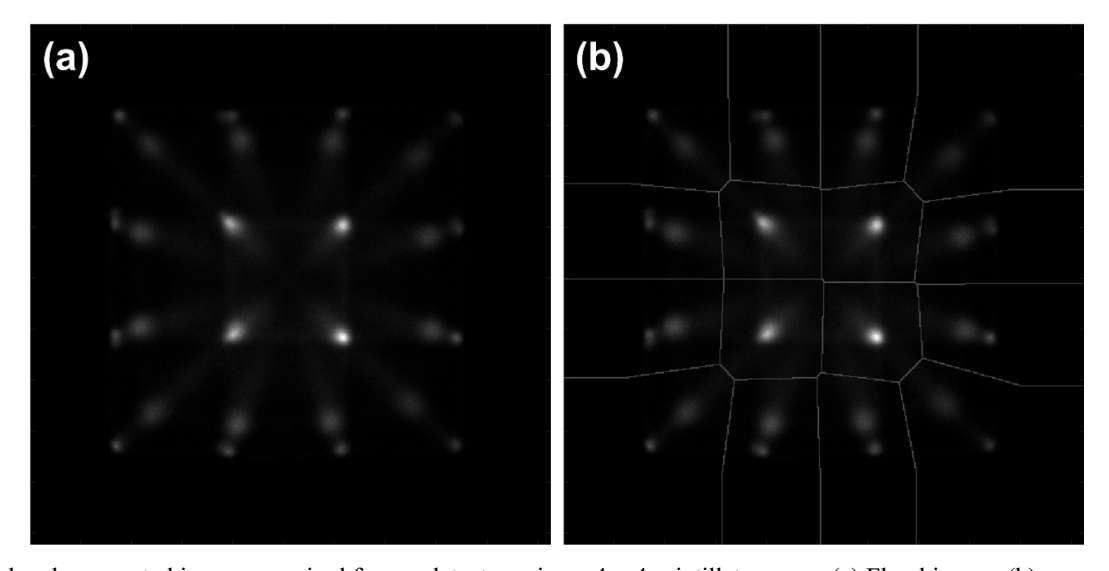
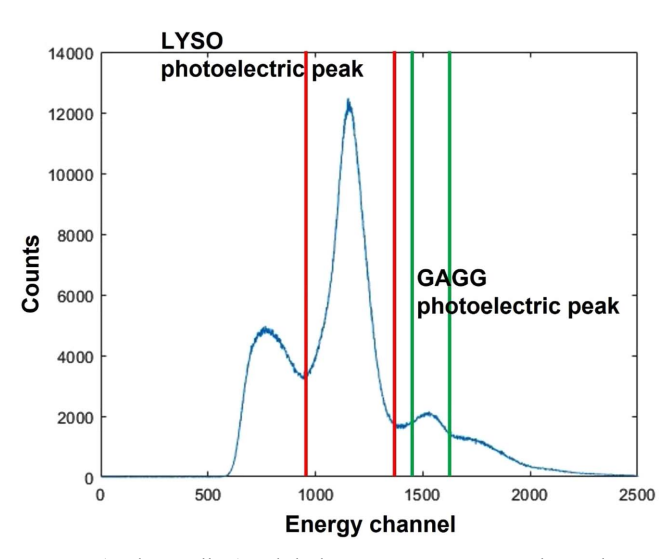


Fig. 3. Flood and segmented images acquired from a detector using a 4 × 4 scintillator array. (a) Flood image, (b) segmented image.

## 3. Results

After constructing the detector, data on gamma-ray interaction were acquired using a Na-22 source. Gamma-rays emitted from the Na-22 radiation source interact with the LYSO and GAGG scintillation pixels of the scintillator block to generate light, which is converted into an electrical signal and collected by the SiPM. Flood images and energy spectra were constructed based on the collected data. Fig. 3 shows flood image and segmented image constructed using all energies. It can be confirmed



**Fig. 4.** (Color online) Global energy spectrum. The red area represents the photoelectric peak area of the Na-22 radiation source measured in LYSO, and the green area represents the photoelectric peak area measured in GAGG.

that a  $4 \times 4$  scintillation pixel array is displayed as an image. Fig. 4 shows the energy spectrum constructed based on all the acquired energies. It can be seen that the photoelectric peak regions appear in two places. The photoelectric peak region on the low channel side is the region acquired from the LYSO scintillator, and the photoelectric peak region on the high channel side is the region acquired from the GAGG scintillator. In other words, since the two types of scintillators form photoelectric peaks in different regions, if they are separated, the DOI layer can be determined. Fig. 5 shows a flood image composed by separating only the energy of the photoelectric peak region formed from each type of scintillator. (a) is a flood image for the LYSO scintillation pixel array, which is the photoelectric peak region on the low channel side, and (b) is a flood image for the GAGG scintillation pixel array, which is the photoelectric peak region on the high channel side. It can be confirmed that the pixels generated at the edge of the flood image of the GAGG scintillation pixel array are more widely distributed. This is considered to be due to the amount of data acquired from the GAGG scintillation pixel and the algorithm applied when forming the flood image. Fig. 6 shows the energy spectrum by region according to the  $4 \times 4$  array partitioning. It can be confirmed that photoelectric peaks are formed in two parts in all regions. In the global energy spectrum, the energy resolution was 22.51% and 17.11% at each photoelectric peak, and the energy resolution in the 4 × 4 partitioning region was an average of 11.49 ± 2.17% for the LYSO scintillator and an average of  $15.38 \pm 3.05\%$  for the GAGG scintillator.

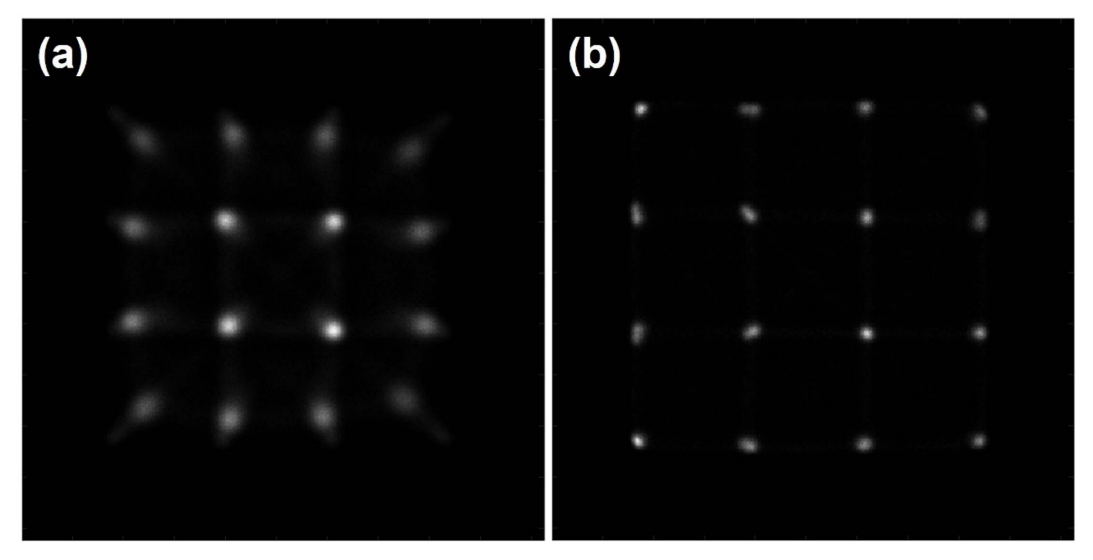


**Fig. 5.** Flood images of each photoelectric peak area. Flood images of (a) LYSO scintillation pixel array, and (b) GAGG scintillation pixel array.

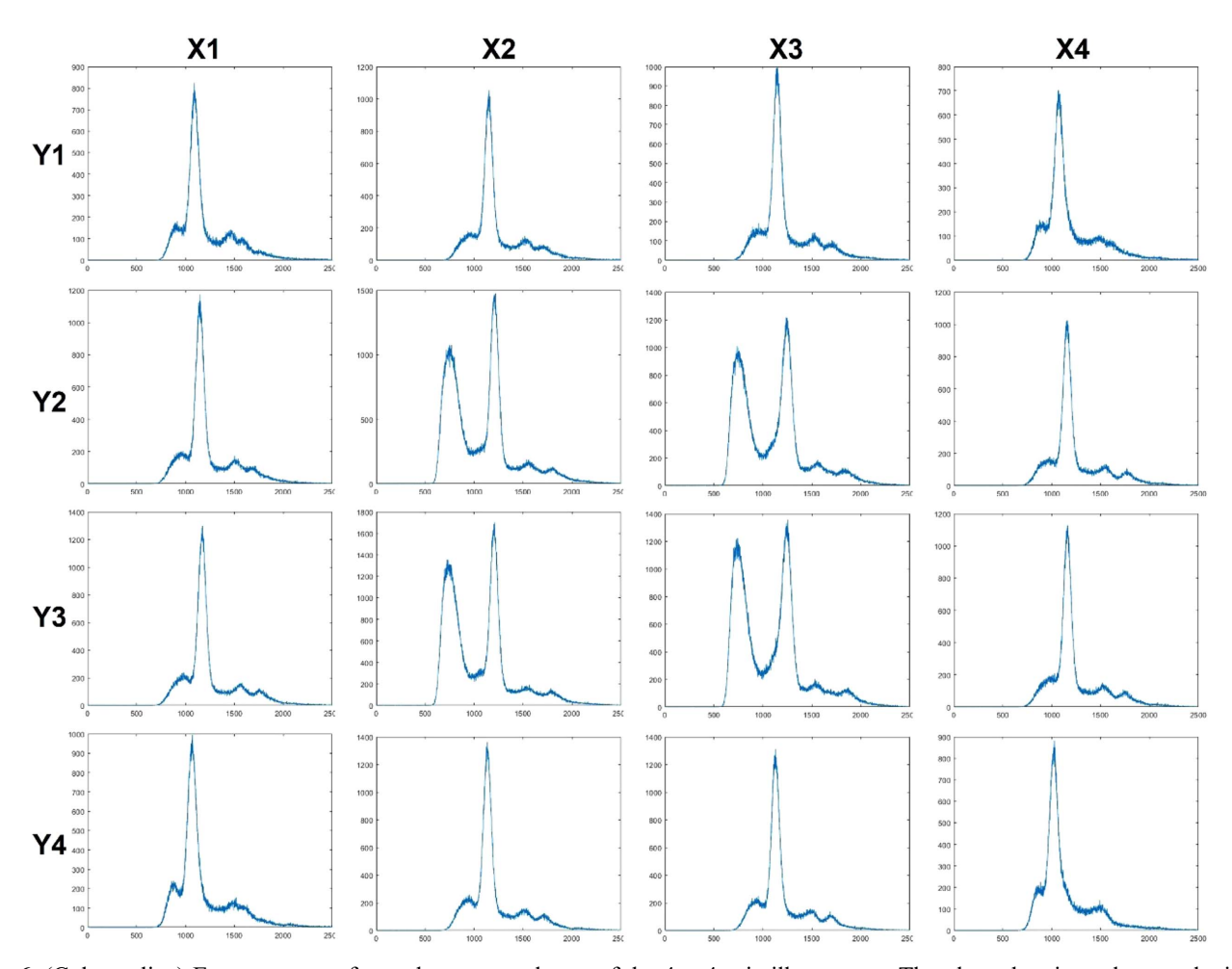


Fig. 6. (Color online) Energy spectra for each segmented area of the  $4 \times 4$  scintillator array. The photoelectric peak area obtained from LYSO and GAGG scintillators are identified in all energy spectra.

## 4. Discussion and Conclusions

We have developed a DOI detector for PET/MRI that operates in a magnetic field. Since the amplification is achieved by moving electrons in a vacuum tube, which is a conventional photosensor, PMT, the signal is distorted when operating in a magnetic field. However, SiPM, a semiconductor photosensor, can operate in a magnetic field without signal distortion, so we developed a detector using it. To evaluate the detector's DOI layer discrimination and performance, gamma-ray interaction was induced by a Na-22 radiation source. The scintillator block of the detector consists of two layers of LYSO and GAGG scintillators, and the layer discrimination was configured based on the characteristics of different scintillators. The GAGG scintillator generates more light than the LYSO scintillator, which causes the signal size to be different, and the positions of the photoelectric peaks in the energy spectrum to be formed differently. It was confirmed that

the DOI layer could be distinguished by obtaining the energy spectrum and separating the photoelectric peak area of the scintillator. Although the DOI could not be distinguished in the acquired flood image, it was possible to obtain flood images of each layer through energy separation. Spatial resolution is important for imaging small animals. Therefore, the smaller the spatial resolution, the better the image can be obtained. To achieve this, very small scintillation pixels must be used, and the DOI layer must be measured. The focus of this study is whether the DOI layer can be measured. Although the scintillator used is not small enough, it can be considered to be large enough to evaluate the possibility of measuring the DOI layer. In the future, we plan to conduct additional study on detectors using smaller scintillators. It is expected that a highresolution DOI measurement system that can operate in a high magnetic field without signal distortion can be developed if a preclinical PET/MRI system is configured using this detector.

# References

- [1] A. D. Van den Abbeele, The Oncologist, 13, 8 (2008).
- [2] M. Ljungberg and P. H. Pretorius, Br. J. Radiol. 91, 20160402 (2018).
- [3] P. Ritt, Semin. Nucl. Med. 52, 276 (2022).
- [4] M. S. Judenhofer and S. R. Cherry, Semin. Nucl. Med. 43, 19 (2013).
- [5] J. Seidel, J. J. Vaquero, S. Siegel, W. R. Gandler, and M. V. Green, IEEE Trans. Nucl. Sci. 46, 485 (1999).
- [6] J. D. Thiessen, M. A. Koschan, C. L. Melcher, F. Meng, G. Schellenberg, and A. L. Goertzen, Nucl. Instrum. Methods Phys. Res. A 882, 124 (2018).
- [7] S.-J. Lee, D.-H. Han, and C.-H. Baek, J. Magn. **26**, 437 (2021).
- [8] G. R. Kim, J. H. Kwak, and S.-J. Lee, J. Magn. **29**, 456 (2024).

- [9] Y. Shao, R. W. Silverman, R. Farrell, L. Cirignano, R. Grazioso, K. S. Shah, G. Vissel, M. Clajus, T. O. Tumer, and S. R. Cherry, IEEE Trans. Nucl. Sci. 47, 1051 (2000).
- [10] Y. Shao, H. Li, and K. Gao, Nucl. Instrum. Methods Phys. Res. A 580, 944 (2007).
- [11] C. S. Levin, IEEE Trans. Nucl. Sci. 49, 2236 (2002).
- [12] A. Vandenbroucke, A. M. K. Foudray, P. D. Olcott, and C. S. Levin, Phys. Med. Biol. 55, 5895 (2010).
- [13] C.-H. Baek and S.-J. Lee, New Phys.: Sae Mulli. **70**, 903 (2020).
- [14] https://www.epic-crystal.com/scintillation-crystals/gaggce-crystal.html.
- [15] https://www.epic-crystal.com/scintillation-crystals/lysocecrystal.html.
- [16] J. Du, J. P. Schmall, Y. Yang, K. Di, E. Roncali, G. S. Mitchell, S. Buckley, C. Jackson, and S. R. Cherry, Med. Phys. 42, 585 (2015).